Photomodulation and Photopumping in Membranes Containing Carriers Optimized for Facilitated Transport in the Dark

Teresa L. Longin and Carl A. Koval*

Department of Chemistry and Biochemistry, University of Colorado, Boulder, Colorado 80309-0215

Richard D. Noble*

Department of Chemical Engineering, University of Colorado, Boulder, Colorado 80309-0215

Received: February 7, 1997; In Final Form: April 18, 1997[⊗]

A steady-state model describing photofacilitated transport in liquid membranes is presented. The model can be used to consider photoactive carriers with a wide range of thermodynamic and kinetic properties in order to calculate photoinduced transport of solutes down their concentration gradient (photomodulation) and against their concentration gradient (photopumping). The description of transport in these systems is generalized by combining the relevant physical constants (diffusion coefficients, rate constants, concentrations, molar absorptivities, light intensity, etc.) into dimensionless parameters. Detailed descriptions of photomodulation and photopumping are presented for the case where the carrier has properties that are optimal for downhill transport in the dark (thermal transport). Absorption of light by the carrier and carrier solute complex can cause downhill transport to increase by 50% or to decrease by a factor of 4 depending on the light intensity. Photopumping can be maintained against a 10-fold concentration gradient. The transport efficiencies for photomodulation and photopumping are also discussed.

Introduction

Facilitated transport in liquid membranes is a rich field of study.[1−3] The general system involves two solutions, the feed and the sweep solution, separated by a layer of immiscible solvent, which constitutes the liquid membrane. The feed solution usually has a high concentration of the solute to be transported, while the sweep solution has a low solute concentration. The immiscible solvent separating the feed and sweep solutions contains a high concentration of a carrier compound, which binds to the solute reversibly and selectively at the feed interface and transports it via diffusion to the sweep interface. Obvious requirements for the efficacy of such systems are that the uncomplexed solute be sparingly soluble in the membrane solvent, while the carrier should be highly soluble in the membrane and sparingly soluble in the feed and sweep solvents. Transport by carrier complexation (thermal transport) can be very large relative to normal diffusion under these conditions.

The possibilities of facilitated transport become much more extensive if the binding properties of the carrier can be modulated with light.[4] In a photofacilitated membrane (depicted in Figure 1), the carrier absorbs light (generally of a fairly narrow bandwidth) and converts to a form that has a low binding affinity for the solute. Shining light of the appropriate wavelength on the sweep interface of the membrane effectively enhances the release rate of solute and thus creates a steep concentration gradient of solute at that interface. This, in turn, increases the total flux of solute across the membrane, a phenomenon referred to as photofacilitation. If the carrier is chemically selective for a particular solute in the feed, the selectivity will be enhanced along with the total flux of solute through the liquid membrane. With light, it might also be possible to maintain active transport against a concentration gradient in a process referred to as photopumping.

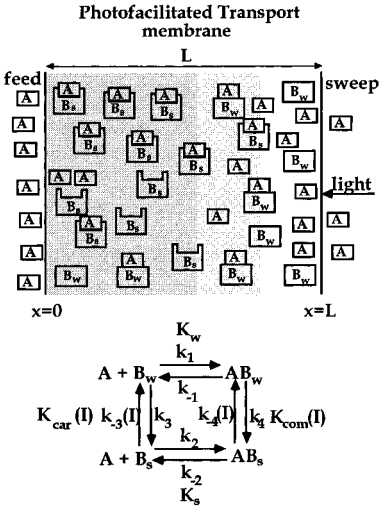

Figure 1. Schematic depiction of a photofacilited liquid membrane and reaction scheme used as the model for photofacilitated transport in liquid membranes.

A number of studies have explored the possibilities of photofacilitated liquid membranes. Systems studied include the transport of hydrogen ions,[5] metal ions,[6−8] organic and inorganic anions,[9,10] and gases.[11] Carriers used include organic bases,[5] thioindigo derivatives,[7] photoactive crown ethers,[8] triaryl cations,[10,9] and spiropyrans.[6] Most of these studies demonstrated photofacilitation and photopumping with varying degrees of success. However, the selection of highly optimal systems for photofacilitation has been hampered by an incomplete understanding of the various parameters important in photofacilitated transport and their relationships to each other.

Jain and Schultz conducted a mathematical analysis of photofacilitated transport using a simplified model.[12] They

[⊗] Abstract published in *Advance ACS Abstracts,* August 15, 1997.

S1089-5647(97)00500-2 CCC: $14.00

based their analysis on the reaction scheme:

$$A + B \underset{k_{-1} + k(I)}{\overset{k_1}{\rightleftharpoons}} AB$$

where A represents the solute, B represents the carrier, and AB represents the carrier−solute complex. They assumed that the decomplexation rate constant for the complex, k_{-1}, was enhanced by the light intensity dependent rate constant $k(I)$. In this model, the principal light dependent parameter was the ratio of the binding constant under illumination to the binding constant in the dark. They further assumed that the illuminated portion of the membrane was completely photobleached and that the dark portion was completely unaffected by the light.

Jain and Schultz demonstrated several very important concepts in their study. They were able to show that both photofacilitation and photopumping should be possible, and they demonstrated the rudimentary relationship between the extent to which the light penetrated into the membrane and the degree of photofacilitation. They explored the determination of photoefficiency in terms of degree of enhancement of transport versus extent of illumination. They also considered photopumping in relation to storage of solar energy.

Clearly, the modeling study carried out by Jain and Schultz was an excellent first step in understanding photofacilitated transport in liquid membranes. However, their study was incomplete in its treatment of the interaction of light with the carrier and complex, making analysis of photoefficiencies unclear. The authors also focused on thermodynamic effects rather than kinetic effects, making comparisons between thermal and light induced rates difficult.

The study reported here incorporates a simple yet physically realistic model for photofacilitation and a more thorough treatment of the interaction of light with the carrier and carrier−solute complex. Both thermodynamic and kinetic parameters are investigated, and the conditions necessary for photofacilitation and photopumping are examined. Transport photoefficiencies for photofacilitation and photopumping are defined and evaluated.

Model

Figure 1 depicts the reaction scheme used as the model for photofacilitated transport in this study. The carrier can exist in the form of four species. The uncomplexed carrier can be in a weakly binding form, B_w, or a strongly binding form, B_s. The carrier−solute complex is either a weakly bound form, AB_w, or a strongly bound form, AB_s.

$$A + B_w \underset{k_{-1}}{\overset{k_1}{\rightleftharpoons}} AB_w \qquad K_w = \frac{k_1}{k_{-1}} \tag{1}$$

$$A + B_s \underset{k_{-2}}{\overset{k_2}{\rightleftharpoons}} AB_s \qquad K_s = \frac{k_2}{k_{-2}} \tag{2}$$

The conversion of weak forms to strong forms is assumed to be a purely thermal process, while the conversions of strong forms to weak forms have both thermal rates (k_{-3} and k_{-4}) and light intensity dependent rates ($k_B(I)$ and $k_{AB}(I)$).

$$B_w \underset{k_{-3} + k_B(I)}{\overset{k_3}{\rightleftharpoons}} B_s \qquad K_{car}(I) = \frac{k_3}{k_{-3} + k_B(I)} \tag{3}$$

$$AB_w \underset{k_{-4} + k_{AB}(I)}{\overset{k_4}{\rightleftharpoons}} AB_s \qquad K_{com}(I) = \frac{k_4}{k_{-4} + k_{AB}(I)} \tag{4}$$

The subscripts "car" and "com" refer to constants for the carrier and complex, respectively, and this notation will be used throughout this report. The constants for binding and interconversion can be considered to be equilibrium constants under dark conditions. Under steady-state illumination, the constants for interconversion will become position dependent.

It is further assumed that B_s and AB_s absorb light of the same wavelength in a narrow range in undergoing conversion to the weak forms and that B_w and AB_w do not absorb light in the same range. While this assumption is made to reduce the number of variables and simplify the calculations, it is not too far from physical reality for many potential carriers. Absorption factors for the weak forms could easily be included in the model for specific cases. The possibility of stimulated emission from the weak forms of the carrier and complex is assumed to be negligible. Finally, the model does not include heating effects due to absorption of light by the membrane.

In this model, the rate constants and the equilibrium constants for the binding of carrier to solute are not directly affected by light. Light does affect the relative concentrations of the strong form and the weak form of the carrier and complex. This enables the separate examinations of thermodynamic and kinetic characteristics. Thus, the important light dependent parameter is not penetration depth (as in the study by Jain and Shultz), but rather the ratios of the light dependent rate constants to the thermal rate constants for interconversion of the strong to weak form of the carrier and complex. The penetration depth of the light results from the incident light intensity and the concentrations of the strong form of the carrier and complex after interaction with light.

The flexibility of this model can be seen in its possible application to real systems. For example, binding of hemoglobin or myoglobin to oxygen or carbon dioxide can be modulated by light.[13] In this case, the strong form of the carrier and the complex are the photochemical ground states, and the weak forms are photoexcited states which have short lifetimes. To represent such a system, K_{car}, K_{com}, and K_s would all be large, and K_w would be small. The introduction of light to the system increases the light dependent rate constants and shifts the concentrations to the weak form of the carrier and complex, ultimately resulting in the release of solute. Since the weak forms are short-lived, this system could be approximated as having only one form of the carrier and complex with the light affecting the binding constant. However, the model presented here requires no such approximation and allows the comparison of light induced rates to thermal rates and an examination of their effect on transport of solute.

The flexibility of the model becomes even more evident when looking at the spiropyran system.[6] In this system, both the strong and weak forms of the carrier and complex are thermally stable, and the direct effect of visible light is to increase the rate of conversion of strong form to weak form. In addition, the thermal interconversion rate constants are so small that the equilibrium limit cannot be assumed. Thus, it is necessary to use a model incorporating all forms of the carrier, complexation and decomplexation rate constants for each form, and rate constants for the interconversion between the forms. Comparisons between thermal rates and light induced rates are crucial for understanding the system.

The model discussed here, while fairly simple, is widely applicable to many real and practical systems. It allows for the existence of different thermodynamically stable forms of the carrier and complex and incorporates comparisons between thermal and light induced rates of conversion.

Mathematical Description

The concentrations of each species in the membrane are controlled by reaction kinetics (as depicted in Figure 1) and by diffusion. According to Fick's second law, at steady state:

$$0 = -k_1[\mathrm{A}][\mathrm{B_w}] - k_2[\mathrm{A}][\mathrm{B_s}] + k_{-1}[\mathrm{AB_w}] + k_{-2}[\mathrm{AB_s}] + D_\mathrm{A}\frac{\mathrm{d}^2[\mathrm{A}]}{\mathrm{d}x^2} \quad (5)$$

$$0 = -k_1[\mathrm{A}][\mathrm{B_w}] + k_{-1}[\mathrm{AB_w}] - k_3[\mathrm{B_w}] + (k_{-3} + k_\mathrm{B}(I))[\mathrm{B_s}] + D_{\mathrm{B_w}}\frac{\mathrm{d}^2[\mathrm{B_w}]}{\mathrm{d}x^2} \quad (6)$$

$$0 = -k_2[\mathrm{A}][\mathrm{B_s}] + k_{-2}[\mathrm{AB_s}] + k_3[\mathrm{B_w}] - (k_{-3} + k_\mathrm{B}(I))[\mathrm{B_s}] + D_{\mathrm{B_s}}\frac{\mathrm{d}^2[\mathrm{B_s}]}{\mathrm{d}x^2} \quad (7)$$

$$0 = k_1[\mathrm{A}][\mathrm{B_w}] - k_{-1}[\mathrm{AB_w}] - k_4[\mathrm{AB_w}] + (k_{-4} + k_\mathrm{AB}(I))[\mathrm{AB_s}] + D_{\mathrm{AB_w}}\frac{\mathrm{d}^2[\mathrm{AB_w}]}{\mathrm{d}x^2} \quad (8)$$

$$0 = k_2[\mathrm{A}][\mathrm{B_s}] - k_{-2}[\mathrm{AB_s}] + k_4[\mathrm{AB_w}] - (k_{-4} + k_\mathrm{AB}(I))[\mathrm{AB_s}] + D_{\mathrm{AB_s}}\frac{\mathrm{d}^2[\mathrm{AB_s}]}{\mathrm{d}x^2} \quad (9)$$

The profile for the light intensity can be calculated from Beer's law in its differential form:

$$\frac{\mathrm{d}I}{\mathrm{d}x} = I(\tilde{E}_{\mathrm{B_s}}[\mathrm{B_s}] + \tilde{E}_{\mathrm{AB_s}}[\mathrm{AB_s}]) \quad (10)$$

where $\tilde{E}_{\mathrm{B_s}}$ and $\tilde{E}_{\mathrm{AB_s}}$ are the molar absorptivity coefficients for the strong form of the carrier and the strong form of the carrier−solute complex, respectively.

If it is assumed that the diffusion coefficients for all forms of the carrier and the complex are the same and do not vary across the membrane, then

$$C_\mathrm{T} = [\mathrm{B_w}] + [\mathrm{B_s}] + [\mathrm{AB_w}] + [\mathrm{AB_s}] \quad (11)$$

where C_T is the total concentration of carrier (both free and complexed) in the membrane. This ensures that the total concentration of carrier is constant across the membrane.

The following boundary conditions apply:

$$\text{at } x = 0, \quad [\mathrm{A}] = [\mathrm{A}]_0, \quad \frac{\mathrm{d}[\mathrm{B_w}]}{\mathrm{d}x} = \frac{\mathrm{d}[\mathrm{B_s}]}{\mathrm{d}x} = \frac{\mathrm{d}[\mathrm{AB_w}]}{\mathrm{d}x} = \frac{\mathrm{d}[\mathrm{AB_s}]}{\mathrm{d}x} = 0 \quad (12)$$

$$\text{at } x = L, \quad [\mathrm{A}] = [\mathrm{A}]_L, \quad \frac{\mathrm{d}[\mathrm{B_w}]}{\mathrm{d}x} = \frac{\mathrm{d}[\mathrm{B_s}]}{\mathrm{d}x} = \frac{\mathrm{d}[\mathrm{AB_w}]}{\mathrm{d}x} = \frac{\mathrm{d}[\mathrm{AB_s}]}{\mathrm{d}x} = 0, I = I_0 \quad (13)$$

Under these conditions, all forms of the carrier are nonvolatile and confined within the membrane. The conditions on A indicate that there is a constant source of A at $x = 0$ (the feed side), and that A is removed from the membrane at $x = L$ (the sweep side) such that the concentration at the sweep interface remains constant. Finally, the boundary condition on the light indicates that the light is incident on the sweep side of the membrane, and the intensity will decay toward the feed side.

In addition, at steady state, the total flux of A is constant across the membrane.

$$J_\mathrm{A} = -D_\mathrm{A}\frac{\mathrm{d}[\mathrm{A}]}{\mathrm{d}x} - D_\mathrm{AB}\frac{\mathrm{d}[\mathrm{AB_w}]}{\mathrm{d}x} - D_\mathrm{AB}\frac{\mathrm{d}[\mathrm{AB_s}]}{\mathrm{d}x} \quad (14)$$

The equations can be converted to dimensionless form to clarify and generalize photofacilitation effects. The dimensionless parameters and variables are

$$\bar{A} = \frac{[\mathrm{A}]}{[\mathrm{A}_0]}, \quad \overline{B_\mathrm{w}} = \frac{[\mathrm{B_w}]}{C_\mathrm{T}}, \quad \overline{B_\mathrm{s}} = \frac{[\mathrm{B_s}]}{C_\mathrm{T}}, \quad \overline{AB_\mathrm{w}} = \frac{[\mathrm{AB_w}]}{C_\mathrm{T}}, \quad \overline{AB_\mathrm{s}} = \frac{[\mathrm{AB_s}]}{C_\mathrm{T}}, \quad \chi = \frac{x}{L} \quad (15)$$

$$\epsilon_\mathrm{w} = \frac{D_\mathrm{AB}}{L^2k_{-1}}, \quad \epsilon_\mathrm{s} = \frac{D_\mathrm{AB}}{L^2k_{-2}}, \quad \epsilon_{\mathrm{car}_0} = \frac{D_\mathrm{AB}}{L^2k_{-3}}, \quad \epsilon_{\mathrm{com}_0} = \frac{D_\mathrm{AB}}{L^2k_{-4}} \quad (16)$$

$$K_\mathrm{w}^\mathrm{d} = \frac{k_1}{k_{-1}}[\mathrm{A}]_0, \quad K_\mathrm{s}^\mathrm{d} = \frac{k_2}{k_{-2}}[\mathrm{A}]_0, \quad K_{\mathrm{car}_0} = \frac{k_3}{k_{-3}}, \quad K_{\mathrm{com}_0} = \frac{k_4}{k_{-4}} \quad (17)$$

$$\alpha = \frac{D_\mathrm{AB}C_\mathrm{T}}{D_\mathrm{A}[\mathrm{A}]_0} \quad (18)$$

The dimensionless parameters and variables involving light are

$$\bar{I} = \frac{I}{I_0} \quad (19)$$

$$\eta_\mathrm{car} = \frac{\Phi_{\mathrm{B_s}}E_{\mathrm{B_s}}I_0}{k_{-3}}, \quad \eta_\mathrm{com} = \frac{\Phi_{\mathrm{AB_s}}E_{\mathrm{AB_s}}I_0}{k_{-4}} \quad (20)$$

$$\epsilon_\mathrm{car}(I) = \frac{D_\mathrm{AB}}{L^2(k_{-3} + k_\mathrm{B}(I))} = \frac{\epsilon_{\mathrm{car}_0}}{1 + \eta_\mathrm{car}\bar{I}}, \quad \epsilon_\mathrm{com}(I) = \frac{D_\mathrm{AB}}{L^2(k_{-4} + k_\mathrm{AB}(I))} = \frac{\epsilon_{\mathrm{com}_0}}{1 + \eta_\mathrm{com}\bar{I}} \quad (21)$$

$$K_\mathrm{car}(I) = \frac{k_3}{k_{-3} + k_\mathrm{B}(I)} = \frac{K_{\mathrm{car}_0}}{1 + \eta_\mathrm{car}\bar{I}}, \quad K_\mathrm{com}(I) = \frac{k_4}{k_{-4} + k_\mathrm{AB}(I)} = \frac{K_{\mathrm{com}_0}}{1 + \eta_\mathrm{com}\bar{I}} \quad (22)$$

$$\beta_\mathrm{car} = \tilde{E}_{\mathrm{B_s}}C_\mathrm{T}L, \beta_\mathrm{com} = \tilde{E}_{\mathrm{AB_s}}C_\mathrm{T}L \quad (23)$$

Here, Φ represents the quantum yield for conversion of strong form of carrier (or complex) to weak form of carrier (or complex) in units of mol of strong form converted/mol of photons absorbed. E represents molar absorptivity in units of cm^2/mol. $\tilde{E}$ represents molar absorptivity in units of L/mol cm. I_0 is the incident light intensity in units of mol of photons/cm^2 s.

The resulting dimensionless equations are

$$\frac{d^2\bar{A}}{d\chi^2} = \frac{\alpha K_w^d}{\epsilon_w}\bar{A}\,\overline{B_w} - \frac{\alpha}{\epsilon_w}\overline{AB_w} + \frac{\alpha K_s^d}{\epsilon_s}\bar{A}\,\overline{B_s} - \frac{\alpha}{\epsilon_s}\overline{AB_s} \quad (24)$$

$$\frac{d^2\overline{B_w}}{d\chi^2} = \frac{K_w^d}{\epsilon_w}\bar{A}\,\overline{B_w} - \frac{1}{\epsilon_w}\overline{AB_w} + \frac{K_{car}(I)}{\epsilon_{car}(I)}\overline{B_w} - \frac{1}{\epsilon_{car}(I)}\overline{B_s} \quad (25)$$

$$\frac{d^2\overline{B_s}}{d\chi^2} = \frac{K_s^d}{\epsilon_s}\bar{A}\,\overline{B_s} - \frac{1}{\epsilon_s}\overline{AB_s} - \frac{K_{car}(I)}{\epsilon_{car}(I)}\overline{B_w} + \frac{1}{\epsilon_{car}(I)}\overline{B_s} \quad (26)$$

$$\frac{d^2\overline{AB_w}}{d\chi^2} = -\frac{K_w^d}{\epsilon_w}\bar{A}\,\overline{B_w} + \frac{1}{\epsilon_w}\overline{AB_w} + \frac{K_{com}(I)}{\epsilon_{com}(I)}\overline{AB_w} - \frac{1}{\epsilon_{com}(I)}\overline{AB_s} \quad (27)$$

$$\frac{d^2\overline{AB_s}}{d\chi^2} = -\frac{K_s^d}{\epsilon_s}\bar{A}\,\overline{B_s} + \frac{1}{\epsilon_s}\overline{AB_s} - \frac{K_{com}(I)}{\epsilon_{com}(I)}\overline{AB_w} + \frac{1}{\epsilon_{com}(I)}\overline{AB_s} \quad (28)$$

$$\frac{d\bar{I}}{dx} = \bar{I}(\beta_{car}\overline{B_s} + \beta_{com}\overline{AB_s}) \quad (29)$$

$$1 = \overline{B_w} + \overline{B_s} + \overline{AB_w} + \overline{AB_s} \quad (30)$$

The dimensionless boundary conditions become

$$\text{at } \chi = 0, \quad \bar{A} = 1, \quad \frac{d\overline{B_w}}{d\chi} = \frac{d\overline{B_s}}{d\chi} = \frac{d\overline{AB_w}}{d\chi} = \frac{d\overline{AB_s}}{d\chi} = 0 \quad (31)$$

$$\text{at } \chi = 1, \quad \bar{A} = \overline{A_1}, \quad \frac{d\overline{B_w}}{d\chi} = \frac{d\overline{B_s}}{d\chi} = \frac{d\overline{AB_w}}{d\chi} = \frac{d\overline{AB_s}}{d\chi} = 0, \quad \bar{I} = 1 \quad (32)$$

A dimensionless flux can also be defined as

$$N_{\bar{A}} = -\frac{d\bar{A}}{d\chi} - \alpha\frac{d\overline{AB_w}}{d\chi} - \alpha\frac{d\overline{AB_s}}{d\chi} \quad (33)$$

Another convenient term for characterizing facilitation is the facilitation factor *F*, defined as the ratio of the total dimensionless flux of A with carrier present to the total dimensionless flux of A without carrier present at the same concentration driving force across the membrane.

$$F = \frac{N_{\bar{A},\text{carrier}}}{N_{\bar{A},\text{no carrier}}} \quad (34)$$

The dimensionless equilibrium constants represent the ratios of the normalized concentrations present. The ϵ's can be considered kinetic terms which relate diffusion times to reaction times. Small ϵ's indicate large rate constants and rapid reaction rates. The η terms are ratios of the maximum light induced rates for conversion of strong form to weak form versus the thermal rates. For a given thermal rate, an increase in η indicates an increase in incident light intensity. Finally, the β terms can be considered as normalized molar absorptivity coefficients.

It is important to note that not all of the parameters are independent of each other. Defining three of the four equilibrium constants is sufficient to determine the fourth. In general, when the dimensionless mass transport equations were solved, K_w^d, K_s^d, and $K_{car}(I)$ were defined and $K_{com}(I)$ was calculated as

$$K_{com}(I) = \frac{K_{car}(I)K_s^d}{K_w^d} \quad (35)$$

In addition, each η term is related to the other through ϵ_{car_0}, ϵ_{com_0}, β_{car}, and β_{com}. Generally, when solving the equations, η_{car}, ϵ_{car_0}, ϵ_{com_0}, β_{car}, and β_{com} were defined and η_{com} was calculated as

$$\eta_{com} = \frac{\Phi_{AB_s}\eta_{car}\epsilon_{com_0}\beta_{com}}{\Phi_{B_s}\epsilon_{car_0}\beta_{car}} \quad (36)$$

Throughout the calculations, Φ_{B_s} and Φ_{AB_s} were set equal to one. Many potential carriers have high quantum yields for conversion, so the approximation of setting Φ_{B_s} and Φ_{AB_s} equal to one is not unreasonable. However, if the quantum yields for conversion are much less than one, then the incident light intensity necessary to achieve a certain effect at a given η_{car} or η_{com} will be proportionally greater.

It is only necessary to solve three of the four dimensionless mass transport equations for the various forms of the carrier, since the mass balance on the carrier can be used to calculate the fourth. Thus, eqs 24, 26−29 were solved, and eq 30 was used to substitute for $\overline{B_w}$. Since second-order coupled differential equations such as these generally do not have analytical solutions, numerical methods are necessary to solve for concentration and flux profiles. The FORTRAN program BVPFD (from the IMSL library) was used to obtain solutions.

This program allows the use of a logarithmic *x* grid, providing points very close together at the edges where gradients are steep. Conversely, the grid is widened in the middle where changes are gradual, providing faster calculations. If necessary, the program BVPFD will insert more *x* points into the grid than were used in the initial guess in order to achieve convergence. To determine the minimum grid resolution necessary to always achieve convergence, various numbers of *x* points were tried in initial guesses until the program always returned solutions with the same number of *x* points as the initial guess. For the series of simulations described in this paper, the *x* grid always contained 151 points. Increasing the number of *x* points in the grid changed the results by less than 0.001%.

The accuracy of the simulations was checked against known solutions for thermal facilitated transport.[14] In this model, thermal-facilitated transport corresponds to an $I_0 = 0$ ($\eta = 0$). Since most modeling studies of facilitated transport involved only one form of the carrier and complex, K_{car_0} was set to 100, which was sufficient to set most of the carrier in the strong forms. Varying thermal parameters such as K_s^d, ϵ_s, and α produced results that were identical with those reported for previous modeling studies.[14]

The program does require a reasonably good initial guess when gradients are steep. Initial guesses for dark conditions ($\eta = 0$) and low light intensity (small η) were based on results for simulations of facilitated transport under purely thermal conditions.[14] As the light intensity was gradually increased (increasing η), results from lower light intensity solutions were used as initial guesses.

Results and Discussion

There are several variables in the model that could significantly affect the extent of photofacilitation and photopumping. To reduce the number of variables, optimal thermal parameters for facilitated transport were used to determine the feasibility and extent of photofacilitation and photopumping in liquid membranes. Such parameters were previously determined by Kemena and Noble[14] and involve small ϵ's (<1), large α (>10),

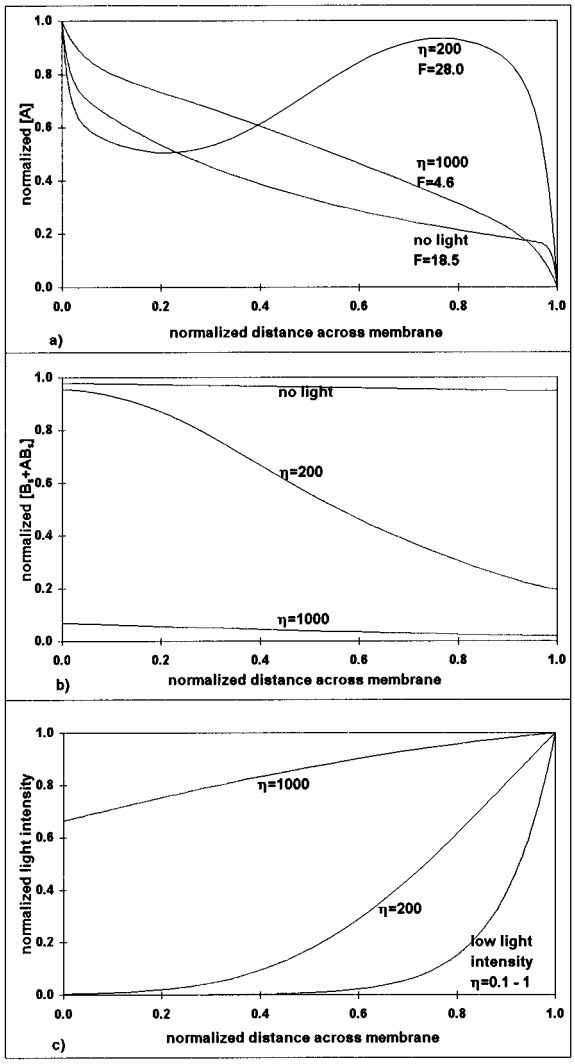

Figure 2. (a) Profiles for normalized concentrations of solute A across the membrane at different incident light intensities. (b) Profiles of the normalized concentrations of total amount of strong form of the carrier and complex (the species which absorb light) across the membrane at different incident light intensities. (c) Profiles of normalized light intensity across the membrane at different incident light intensities.

and a $K_s^d = 5$. For the results discussed below, $\epsilon_s = \epsilon_w = 0.01$, $\epsilon_{car_0} = \epsilon_{com_0} = 0.01$, $\alpha = 50$, $K_s^d = 5$, $K_w^d = 0.05$, $K_{car_0} = 10$, $K_{com_0} = 1000$, and $\beta_{car} = \beta_{com} = 10$, unless otherwise specified. Using these parameters, $\eta_{car} = \eta_{com}$. The focus in this study was on examining the effects of kinetics and light intensity on the photomodulation and photopumping ability of a liquid membrane.

Photofacilitation. Figure 2 shows results for simulations of photofacilitation where the normalized concentration of solute at the sweep interface, $\overline{A_1}$, was set equal to zero. Figure 2a depicts the normalized concentration profiles for A across the membrane. Under dark conditions ($\eta = 0$), a reasonably high facilitation factor of 18.5 was observed, which was consistent with previous models for facilitated transport under similar thermal conditions.[14] As the light intensity was increased, the facilitation factor also increased until it reached a maximum of 28.0 at $\eta = 200$. Increasing the light intensity beyond $\eta = 200$ caused a decrease in the facilitation factor until F reached a final value of 2.8 at $\eta = 10\,000$. Further increases in light intensity beyond $\eta = 10\,000$ did not result in a further significant reduction of the facilitation factor.

The reason for this can be seen in Figure 2b, which depicts the normalized concentration profiles for the sum of B_s and AB_s (the two species that absorb light) across the membrane. For $\eta = 1000$, the total concentration of absorber was less than 10% of the dark value throughout the membrane, indicating nearly photobleached conditions. At this light intensity, the majority of the carrier was in the weak binding form, with the corresponding facilitation factor for that binding constant. For $\eta = 10\,000$, photobleaching was essentially complete, and almost all the carrier was in the weak form. Since the weak binding form is not affected by light, further increases in light intensity did not have an effect on transport once the membrane was photobleached.

It is interesting to examine the qualitative relationships between the concentration profiles for A, B_s, AB_s, and the light intensity for $\eta = 200$, the optimal photofacilitation condition. Figure 2a shows that the concentration gradient for A was very steep close to each interface, indicating very high flux of uncomplexed A into and out of the membrane. About two-thirds of the way through the membrane, there was an increase in the concentration of A, due to photoconversion of AB_s to AB_w and subsequent decomplexation. As can be seen in Figure 2b, the total normalized concentration of absorber dropped significantly in the third of the membrane closest to the sweep interface. As shown in Figure 2c, although the light penetrated through the entire membrane, the intensity dropped close to zero at the feed interface. The overall effect was a high enough concentration of the strong form of the carrier at the feed interface to draw large amounts of A into the membrane. The light intensity was high enough to significantly photobleach the membrane close to the sweep interface, resulting in a large increase in the concentration of uncomplexed A and a correspondingly large flux of A at the sweep interface.

Photopumping. Figure 3 shows the results for simulations where $\overline{A_1}$ was one or more. This condition represents transport against a concentration gradient, also known as photopumping. Interestingly, the optimal light intensity for photopumping corresponded to η's greater than 200, even though such light intensities had rather poor facilitation factors for $\overline{A_1} = 0$. Characterizing the extent of photofacilitation during transport against a concentration gradient requires the definition of a new facilitation factor, since transport against a concentration gradient cannot occur without carrier. Hence, a new facilitation factor F' is defined as

$$F' = \frac{N_{\bar{A},\eta,\bar{A}_1}}{N_{\bar{A},\mathrm{dark},0}} \tag{37}$$

where $N_{\bar{A},\eta,\bar{A}_1}$ indicates the dimensionless flux of uncomplexed A for a given light intensity parameter and a given normalized sweep concentration of A. Similarly, $N_{\bar{A},\mathrm{dark},0}$ indicates the dimensionless flux of uncomplexed A in the dark with a sweep concentration for A of zero.

As can be seen in Figure 3a, with an $\eta = 600$, transport could be achieved with a sweep concentration of A more than 10 times greater than the feed concentration. Transport against even greater concentration gradients could be achieved with higher light intensities. It is interesting to note that for $\overline{A_1} = 2$, an η of 600 resulted in an F' of 1.00, even though F' was only 0.38 for $\overline{A_1} = 0$.

The explanation for this unexpected trend can be seen in the profiles for the strong forms of the carrier, as shown in Figure 3b. For $\overline{A_1} = 0$, an $\eta = 600$ resulted in a heavily photobleached membrane. However, as the sweep concentration of A increased, the overall chemical equilibrium shifted greatly toward the strong form of the complex, countering the effect of the light. The increase in the strong form of the complex

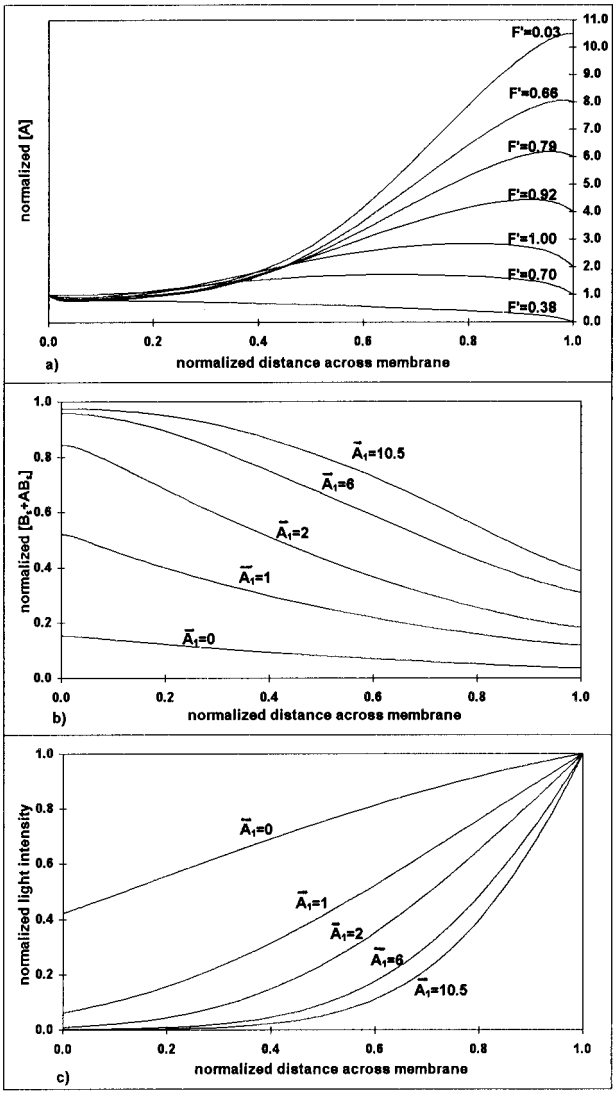

Figure 3. (a) Profiles for normalized concentrations of A across the membrane as a function of increasing normalized concentrations of A at the sweep interface. All profiles are for $\eta = 600$ and $\beta = 10$. The value F' is defined by eq 37 in the text. (b) Profiles for total concentration of strong form of carrier and complex across the membrane at increasing normalized concentrations of A at the sweep interface. The value of $\bar{A}_1$ indicates the normalized concentration of A at the sweep interface. (c) Profiles for normalized light intensity across the membrane as a function of increasing normalized concentrations of A at the sweep interface.

also resulted in an increase in the transport of A. The light profiles depicted in Figure 3c show that the light intensity dropped to nearly zero about 80%−90% of the way through the membrane for high sweep concentrations of A, while there was significant light intensity at the feed side when the sweep concentration of A was zero. Like the results for photofacilitation, this indicates that optimal conditions for photopumping or photofacilitation result when the light can penetrate through most of the membrane but the intensity goes to zero at the feed interface. This effect did not continue for light intensities greater than $\eta = 1000$. At very high light intensities, the photoinduced rate of conversion of strong form to weak form was sufficient to overcome the increase in strong form of the complex due to high concentrations of A and thoroughly photobleach the membrane.

This effect has interesting ramifications for real systems. For example, imagine a photofacilitated transport membrane operating under optimal thermal parameters with a solute concentration of zero at the sweep interface. Under steady-state illumination

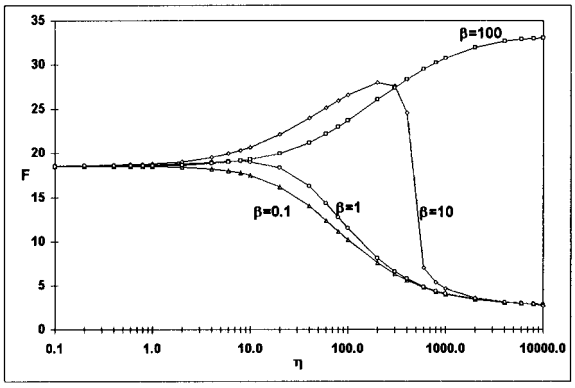

Figure 4. Values of facilitation factor F as a function of η for different normalized absorbtivities, β. The open squares indicate values of F for $\beta = 100$, open diamonds indicate $\beta = 10$, open circles indicate $\beta = 1$, and open triangles indicate $\beta = 0.1$.

at a light intensity equivalent to an η between 200 and 1000, the flux would be expected to increase to a maximum as solute is depleted from the feed solution and concentrated in the sweep solution, and the concentration of strong form of the carrier increases. Eventually, the flux would decrease to zero as the solute concentration at the sweep interface increased. Such a trend is unprecedented in facilitated transport systems and would not necessarily be predicted without a complete modeling study.

The effect of the magnitude of β, the normalized molar absorptivity coefficient, on photofacilitation was also examined. Figure 4 shows the dependence of the facilitation factor on light intensity for various β's. Each point represents the results for a simulation carried out at a particular η, with interconnecting lines which are intended to act as a guide to the eye. In some cases, rapid changes in facilitation occurred with fairly small changes in η.

For small β ($\beta = 0.1$ and $\beta = 1$), there was little or no photofacilitation since light could penetrate well into the membrane and deplete the concentration of strong form of carrier on the feed side of the membrane. Even low light intensities resulted in photobleaching at the feed interface and a reduction in facilitation factor. For $\beta = 10$, fairly small increases in light intensity past the optimal light intensity factor of $\eta = 200$ resulted in a rapid decline in facilitation. At the higher light intensities, light penetrated all through the membrane, resulting in a significant depletion of strong forms of the carrier and complex at the feed interface, greatly reducing the transport properties of the membrane.

For $\beta = 100$, most of the light was absorbed very close to the sweep interface, resulting in photobleaching close to the sweep interface but not in the remainder of the membrane. Even at $\eta = 10\,000$, only half the membrane was photobleached, and high facilitation factors were observed. Transport against normalized sweep concentrations of A greater than ten was also possible at $\beta = 100$. Thus, it appears that for typical membrane thicknesses of 10−100 μm and total carrier concentrations of 0.01−0.1 M, high molar absorptivity coefficients (10^4−10^6 M^{-1} cm^{-1}) are required for photofacilitation and photopumping.

Truly optimal systems for photofacilitation and photopumping would be photoefficient, providing large solute fluxes at low light intensity. A transport photoefficiency can be defined as

$$\Psi = \left(\frac{(\text{total flux A})_{\text{light}} - (\text{total flux A})_{\text{dark}}}{I_0} \right) \times 100 \quad (38)$$

In the dimensionless parameters used in this study, the photoefficiency becomes

$$\Psi = \frac{\beta_{\mathrm{com}}\epsilon_{\mathrm{com}_0}}{\alpha\eta_{\mathrm{com}}}(N_{\bar{A},\mathrm{light}} - N_{\bar{A},\mathrm{dark}}) \times 100 \qquad (39)$$

Under this definition, photoefficiencies can be negative, indicating reduced transport in the light. It should be noted that these photoefficiencies are different from quantum yields in that they are defined using the total incident light, rather than the total absorbed light. For cases where all the light is absorbed in the membrane, transport photoefficiencies are equivalent to quantum yields. For cases where light penetrates through the membrane, quantum yields could be determined by integrating the absorbed light.

Figure 5a shows photoefficiencies versus η for various β's. At $\beta = 0.1$, the photoefficiencies were so low as to be indistinguishable from zero at all light intensities. Higher β's resulted in greater photoefficiencies; however, the photoefficiencies dropped to nearly zero at high light intensities regardless of β. For $\beta = 1$ and $\beta = 10$, photoefficiencies became slightly negative. Note that, for $\beta = 10$, the photoefficiency for $\eta = 200$ (where flux was greatest) was very low and significantly less than at $\eta = 10$. Indeed, for both $\beta = 10$ and $\beta = 100$, the photoefficiencies began falling off rapidly above $\eta = 10$. Thus, the optimal light intensity for photofacilitation does not necessarily provide the most efficient use of light.

Figure 5b shows photoefficiency versus normalized sweep concentration of A for two light intensities that could attain significant photopumping. At $\eta = 1000$, transport could be achieved against a higher concentration gradient than for $\eta = 600$, but the photoefficiencies were generally much lower. Indeed, at the lower normalized sweep concentrations of A, the photoefficiencies for $\eta = 1000$ were less than zero. At $\eta = 1000$, the light intensity was sufficiently high to convert most of the strong forms of the carrier and complex to the weak forms throughout the membrane, resulting in poorer transport under illumination than in the dark. At the higher normalized sweep concentrations of A, there was sufficient free solute in the membrane to drive the binding equilibria toward formation of the strong form of the complex, as described above. This resulted in facilitation factors under illumination that were slightly greater than those in the dark and also resulted in low but positive photoefficiencies. Light intensities above $\eta = 2000$ resulted in significant photobleaching and reduced transport, regardless of the normalized sweep concentration of A. Thus, for any sort of practical applications, the most efficient system might involve transport against a fairly low concentration gradient, which could be maintained with relatively low light intensities.

All the photoefficiencies obtained in this study were quite low (<0.2%), even for high β. This is not surprising since the conditions used provided optimal thermal transport, and the addition of light would not be expected to have a great effect. Higher photoefficiencies as well as greater photofacilitation effects would be expected for thermal conditions that are far from optimal. Further studies are being carried out to explore the effects of nonoptimal thermal parameters, such as large K_s^d and slow kinetics, on photofacilitation. The eventual goal of these studies is to determine the optimal physical parameters and conditions for photofacilitation and photopumping. Once the optimal parameters are determined, they can be compared to the actual parameters used in various photofacilitated transport membranes to suggest how such real systems could be improved or whether one would expect any photofacilitation at all.

Conclusions

A model has been developed for photofacilitated transport through liquid membranes. The model incorporates a weak and a strong form of the carrier and complex and takes into account rates for interconversion between the forms as well as rates of complexation and decomplexation. Light influences the relative concentration of strong forms of the carrier and complex versus the weak forms by enhancing the rate constants for conversion of the strong to the weak forms. This model is quite general, applying to systems in which the weak forms of the carrier and complex are short-lived photoexcited states, as well as systems where both the strong and weak forms of carrier and complex are thermally stable.

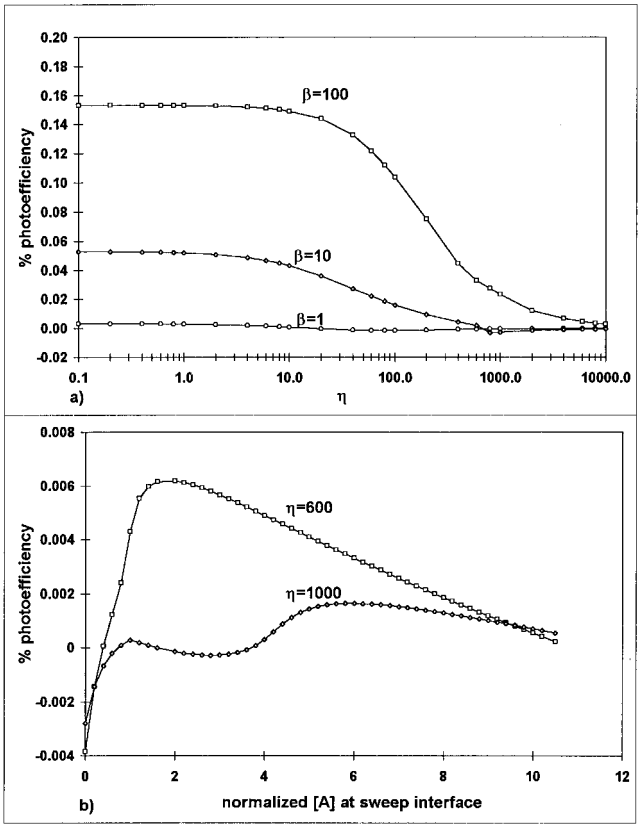

Figure 5. (a) Photoefficiency as a function of η for different β's. Open squares indicate photoefficiency values for $\beta = 100$, open diamonds indicate $\beta = 10$, and open circles indicate $\beta = 1$. Values for $\beta = 0.1$ are not shown, as they are so small as to be indistinguishable from zero on the scale of the graph. (b) Photoefficiency as a function of normalized concentration of A at the sweep interface for $\eta = 600$ and $\eta = 1000$, $\beta = 10$. Open squares indicate photoefficiency values for $\eta = 600$, and open diamonds indicate $\eta = 1000$.

This study suggests that both photofacilitation and photopumping are possible with systems that are optimal for thermal facilitated transport. High molar absorptivities and high total carrier concentrations (i.e., 10^5 M^{-1} cm^{-1} or greater for total carrier concentrations of 0.01 M) are required to obtain either phenomenon. Results suggest that it is possible to obtain a 50% increase in facilitation under illumination versus facilitation in the dark, but that the facilitation effect falls off rapidly at light intensities higher than the optimal value. It is also possible to pump against a greater than 10-fold concentration gradient with a light intensity slightly higher than that which was optimal for photofacilitation. Again, the effect is dependent on light intensity—too great an intensity reduces the ability of the membrane to pump against a concentration gradient.

There is a balance between light intensity and thermal rates of interconversion between forms. At the light intensity for greatest photofacilitation, there is a significant concentration of strong form of the carrier and complex at the feed interface, while the concentration falls off significantly within about 25%−50% of the sweep interface. This corresponds to a light profile

in which the light penetrates most of the way across the membrane but drops to nearly zero at the feed interface. Increasing the light intensity even slightly beyond the optimal value causes significant decreases in the concentrations of the strong forms of the carrier and complex at the feed interface with a resulting reduction in facilitation.

An analysis of photoefficiencies indicates that the highest facilitation is not necessarily the most efficient. In general, the most photoefficient light intensities were well below those resulting in the greatest degree of photofacilitation. Thus, in choosing a system, there will be a tradeoff between high flux and maximum efficiency.

This study focused on membranes in which the strong forms of the carrier and complex were optimized for thermal transport. Obviously, this applies to only a few systems; none of those mentioned in the introduction were optimized for thermal transport. Further studies are being conducted to explore a greater range of membrane parameters and determine those that provide the highest degrees of photofacilitation and photoefficiency. In addition, this model can be used to study membranes in which the light converts the weak form of the membrane to the strong form, a case which has rarely been studied.

Acknowledgment. The authors thank Professor David E. Clough for many extremely useful discussions. This work was funded by the Department of Energy (BES) Solar Photochemistry Program, Grant DE-FG03-94ER14434.

References and Notes

(1) Halwachs, W.; Schügerl, K. *Int. Chem. Eng.* **1980**, *20*, 519.
(2) Way, J. D.; Noble, R. D.; Flynn, T. M.; Sloan, E. D. *J. Membr. Sci.* **1982**, *12*, 239.
(3) Meldon, J. H.; Stroeve, P.; Gregoire, C. E. *Chem. Eng. Commun.* **1982**, *16*, 263.
(4) Schultz, J. S. *Science* **1977**, *197*, 1177.
(5) Haberfield, P. *J. Am. Chem. Soc.* **1987**, *109*, 6178.
(6) Shimidzu, T.; Yoshikawa, M. *J. Membr. Sci.* **1983**, *13*, 1.
(7) Irie, M.; Kato, M. *J. Am. Chem. Soc.* **1985**, *107*, 1024.
(8) Shinkai, S.; Shigematsu, K.; Sato, M.; Manabe, O. *J. Chem. Soc., Perkin Trans. 1* **1982**, 2735.
(9) Ino, M.; Otsuki, J.; Araki, K.; Seno, M. *J. Membr. Sci.* **1994**, *89*, 101.
(10) Sasaki, H.; Ueno, A.; Osa, T. *Bull. Chem. Soc. Jpn.* **1988**, *61*, 2321.
(11) Jain, R.; Schultz, J. S. *J. Membr. Sci.* **1986**, *26*, 313.
(12) Jain, R.; Schultz, J. S. *J. Membr. Sci.* **1983**, *15*, 63.
(13) Bonaventura, C.; Bonaventura, J.; Antonini, E.; Brunori, M.; Wyman, J. *Biochemistry* **1973**, *12*, 3423.
(14) Kemena, L. L.; Noble, R. D.; Kemp, N. J. *J. Membr. Sci.* **1983**, *15*, 259.